Effect of Nitrogen Adsorption on the Mid-Infrared Spectrum of Water Clusters

Waldemar Hujo,[†] Michael Gaus,[‡] Markus Schultze,[†] Tomáš Kubař,[‡] Jörg Grunenberg,[§] Marcus Elstner,*[‡] and Sigurd Bauerecker*[†]

[†]Institut für Physikalische und Theoretische Chemie, Technische Universität Braunschweig, Hans-Sommer-Strasse 10, D-38106 Braunschweig, Germany

[‡]Institute of Physical Chemistry, Karlsruhe Institute of Technology, Kaiserstrasse 12, 76131 Karlsruhe, Germany

[§]Institut für Organische Chemie, Technische Universität Braunschweig, Hagenring 30, 38106 Braunschweig, Germany

S *Supporting Information*

ABSTRACT: Experimental Fourier-transform infrared spectra and DFT calculated infrared spectra are compared to investigate the effect of adsorbed nitrogen on the OH-stretch band complex of water clusters. Using a collisional cooling experiment, pure as well as partially and completely N_2-covered water clusters consisting of 20–200 water molecules have been generated in thermal equilibrium in the aerosol phase within the temperature range of 5–80 K. Computational IR-spectra simulations have been performed for discrete pure and N_2-covered water clusters including 10, 15, 20, and 30 water molecules. The adsorbed N_2 molecules especially affect the three-coordinated water molecules at the cluster surface which could be observed as a blue shift of the companion O—H band at 2900 cm^{-1} and a red shift of the dangling O—H band at 3700 cm^{-1} by about 20 cm^{-1} in both cases.

The most striking effect of the N_2 adsorbate is an intensity increase of the dangling O—H band by a factor of 3–5. Furthermore, the onset temperature of nitrogen adsorption at the water cluster surface was experimentally found to be roughly 30 K for cluster sizes of about 100 water molecules. Experimental and computational results are in good agreement. The presented results are based on and support the work of V. Buch, J. P. Devlin, and co-workers (e.g., *J. Phys. Chem. B*, 1997; *J. Phys. Chem. A*, 2003; *Int. Rev. Phys. Chem.*, 2004).
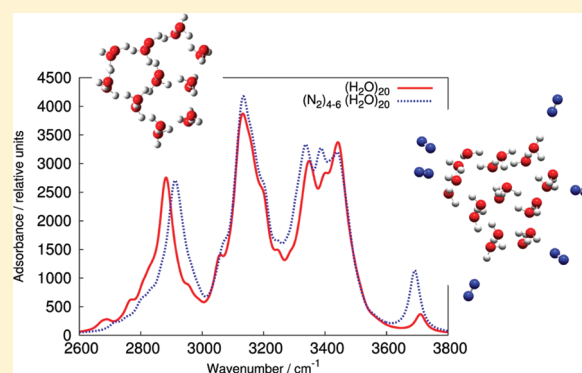
■ INTRODUCTION

Water clusters in the aerosol phase have become an important branch of H_2O research and are a subject of considerable research interest of both the experimental and the computational physical chemistry. It is especially the interaction of water clusters with small molecules as dinitrogen that is important for chemical reactions on icy surfaces. In fact, the effect of weak bonding on the vibrational bands of molecules has been known for a long time. For years, this phenomenon has been used to probe the local environment of molecules in clusters, matrices, and solutions as well as on surfaces.[1] One suited experimental method is Fourier-transform infrared (FTIR) spectroscopy, which makes it possible to obtain information on the size, shape, and structure of water clusters based on a vibrational mode analysis.

Typically, weak adsorbates on the surface of water ice cause a red shift of the free OH band of the water molecules by 10–70 cm^{-1}. The magnitude of the red shift depends on the adsorbates and increases in the order CF_4, H_2, Ar, N_2, O_2, CH_4, NO, CO, O_3, and ethylene.[2−4] In this work, we concentrate on the effect of adsorbed N_2.

In previous combined experimental and computational studies, the complex of a single water molecule coordinated to a dinitrogen molecule $(N_2)(H_2O)$ was investigated.[2] Infrared spectra were calculated using ab initio methods and the symmetric and antisymmetric free OH (dangling OH) band to be red shifted by 8 and 10 cm^{-1} with respect to the water monomer, while the intensity of the symmetric and antisymmetric band increased by factors of 4.9 and 2.1, respectively. Further theoretical investigations of this system[5] using MP2 and Monte Carlo calculations revealed that the bonding is mainly dominated by electrostatic interaction between N_2 quadrupole and the asymmetric charge distribution on the water molecule. A substantial contribution of dispersion is present as well. Experimental measurements on the system of dinitrogen adsorbed on amorphous and crystalline ice surfaces revealed red shifts of the dangling OH band of 17 and 22 cm^{-1} and increases of intensity by factors of 1.6 and 1.4.[2] However, the experimental results by Kuma et al.[6] for the $(N_2)(H_2O)$ system

show a red shift of about 5 cm^{-1} for both bands and increase of intensity by factors of 1.9 and 1.3 for the symmetric and antisymmetric bands, respectively. Here, the infrared (IR) spectra were obtained with the helium droplet technique. Furthermore, small uncoated clusters of up to 10 water molecules $(H_2O)_{10}$ were subject of experimental and theoretical IR studies by Buck, Sadlej and Buch et al.[7,8] They computed the vibrational frequencies at a semiempirical level of theory and measured IR spectra of the OH stretch band with the IR depletion technique[9,10] for clusters composed of 8, 9, and 10 water molecules. The measured and calculated spectra are in a good agreement. In ref 8 ab initio and semiempirical calculations were carried out for clusters of 6 and 10 water molecules. DFT calculations were carried out by Xantheas[11] for water clusters in the range $(H_2O)_{1-6}$ which were found to be in excellent agreement to MP2 data. In the size range of $(H_2O)_{2-30}$ water clusters, Hartke[12-14] investigated the structural evolution of the size of these water clusters using TIP4P[15] and TTM2-F.[16] He describes small clusters of this range to be completely part of the surface of the clusters ("all-surface"). As the number of water molecules increases a single water molecule builds a 4-fold coordination in the center of the cluster ("water-centered cage"). In a later study Lagutschenkov and co-workers[17] confirmed his findings by electronic structure computations using MP2 and DFT-B3LYP functional and IR spectra. Low-energy structures of bigger water cluster composed of 20—22, 48, 123, and 293 molecules were calculated by Kazimirski and Buch.[18] They employed the classical TIP4P water model and made use of molecular dynamics simulations (simulated annealing), hydrogen network improvement, and rigid-body diffusion Monte Carlo optimization.

At present, computational studies in the field of electronic structure methods use ab initio or density functional theory (DFT) methods. The former are based on the wave function correlation methods and provide very accurate results up to spectroscopic accuracy; however, their use is limited to systems of small number of atoms due to the high computational cost. On the other hand, DFT calculations make systems of 1000 (and more) atoms accessible, still providing a reasonable accuracy for many properties of interest. In this work, we address the spectroscopic properties of large water—dinitrogen clusters; therefore, DFT is the only viable computational choice. Recently, it has been documented that several semilocal DFT functionals describe hydrogen bonding quite accurately. For example, the DFT-PBE functional allows to compute interaction energies within the accuracy of 1 kcal/mol.[19,20] On the other hand, it is well-known that the DFT-GGA functionals fail to describe van der Waals (VdW) interactions properly. A popular ad hoc solution of this problem is the augmentation of the DFT-GGA energy with an empirical dispersion correction.[21-24] Such corrections are indispensable in order to describe the dispersive interaction of large molecules with DFT accurately. However, for smaller H-bonded complexes, the situation is not so clear as there is still a considerable overlap of electron density of the interacting molecules, and the DFT correlation functional covers a non-negligible part of the interaction. In the case of such VdW complexes, modified DFT functionals can be applied with reasonable success.[25-27] Similarly, based on the study of interaction of small molecules, it was proposed that the BHandH functional is also able to capture the VdW interactions with reasonable accuracy.[28] Here, care should be taken as the results are mostly not transferable to arbitrary complexes. However, once tested for a particular class of

molecular complexes thoroughly, these functionals may be applied to these systems.

In this work, we compare experimental and DFT-calculated IR spectra for dinitrogen-coated clusters of up to 30 water molecules. In a first step, we evaluate several DFT functionals with respect to the relevant properties of these clusters. Then the computed spectra for the larger clusters are used to interpret the experimental data. Of particular interest are the dangling O—H bonds on the surface of water clusters—those that are not involved in direct hydrogen bonds with other water molecules.

■ METHODS

Experimental Methods. The water nanoparticles were formed in a long-path collisional cooling cell which is described in detail in refs 29—31. The cooling system involves a multiple-pulse sample-gas injection device for the generation of molecular nanocomposites,[30,32,33] which is used for single and repetitive pulse injection of the H_2O/He sample gas mixtures, in this work. The IR spectra were recorded with a Nicolet Magna 550 spectrometer equipped with a Globar light source, a KBr beam splitter, KBr windows, and an external InSb detector. Optical path lengths of 12.5 and 15 m were used, and the optical resolution was 4 cm^{-1}. Temperatures were adjusted between 80 and 5 K, i.e., far below 120—140 K, which is the upper temperature range in which the onset of the free OH band occurs spectroscopically.[34,35] The He buffer-gas pressure in the cooling cell varied between 80 and 5 mbar; the nitrogen partial pressure was below 0.1 mbar. The Fourier-transform infrared (FTIR) spectra were recorded in the spectral range 1850—7400 cm^{-1} using a zero filling level of two and Happ—Genzel apodization. The water sample—gas concentration was (a) preadjusted as a mixture with helium (91 ppm H_2O/He and 1.43 ppm H_2O/He, certified by Messer Griesheim) or (b) regulated by a helium gas flow that took the water vapor from a porous adsorber or (c) from a temperature-adjusted cryocooler source.[33] Note that the water sample—gas concentration which finally enters the cooling cell cannot accurately be determined due to exchange processes with the involved surfaces. Nevertheless, the water concentration can continuously be reduced toward zero by flushing with helium gas as by use of technique (b). The main parameter which determines the water particle size is the temperature. Lower temperatures cause smaller critical nuclei and therefore more and smaller particles.

Computational Methods. In a first step, we investigated the performance of several gradient corrected and hybrid density functionals in the description of hydrogen-bonding interaction energies and vibrational frequencies of small water—dinitrogen complexes. We are testing the popular functional B3LYP,[37] BHandH,[38] which was proposed to work well for this kind of system,[28] and PBE,[39] which was shown to perform well for hydrogen-bonded complexes.[19,20,40,41] Corrections for neither the basis set superposition error (BSSE)[42] nor the anharmonic effects are feasible for such large molecular systems. To estimate the magnitude of the error at least for BSSE, we consider the counterpoise correction in our benchmark calculation. All calculations were performed with the Gaussian03 package.[43]

DFT calculations were carried out on clusters composed of 10, 15, 20, and 30 water molecules, which we denote as $(H_2O)_{10}$, $(H_2O)_{15}$, $(H_2O)_{20}$, and $(H_2O)_{30}$, respectively. For each cluster size, we used the first 10 lowest-energy structures yield by the conformational search with the empirical TIP4P water model.[18]
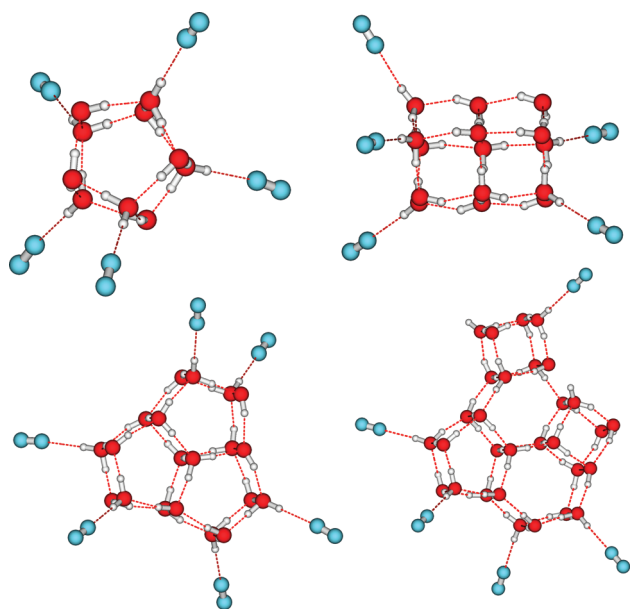
6219

dx.doi.org/10.1021/jp111481q |*J. Phys. Chem. A* 2011, 115, 6218–6225

Figure 1. N_2-coated clusters $(H_2O)_{10}$, $(H_2O)_{15}$, $(H_2O)_{20}$, and $(H_2O)_{30}$.
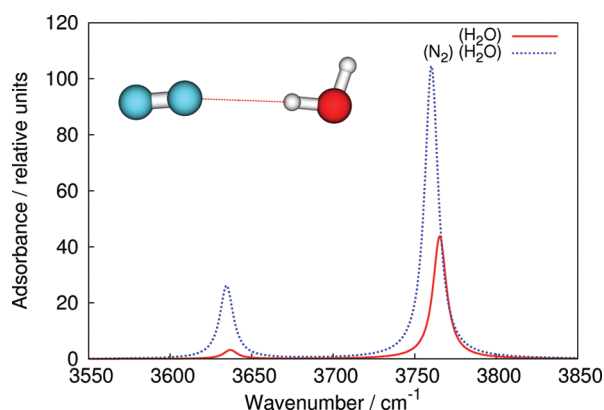

Figure 2. The test system $(N_2)(H_2O)$ and its IR spectrum calculated at the PBE/6-311+G(d,p) level of theory.

The water molecules within these clusters form an internal network of hydrogen bonds, nevertheless there are several free O—H groups at the surface being not involved in any hydrogen bonding. We constructed the models of N_2-coated water clusters by adding N_2 molecules at these sites, as shown in Figure 1. Obviously, the key parameters describing these systems are the internal hydrogen bonding interactions and the N_2—water interactions. Of particular interest is the change of the O—H vibrational modes upon N_2 binding.

In order to benchmark the selected DFT functionals for this purpose, we performed calculations on the $(N_2)(H_2O)$ complex; see Figure 2.

The geometry of the model system was optimized at the PBE/6-311+G(d,p), B3LYP/6-311+G(d,p), BHandH/6-311+G(d,p), and MP2/6-311+(d,p)[44] levels of theory (in gas phase at 0 K), followed by the calculation of the IR spectrum using the normal-mode analysis for each optimized structure. The spectrum obtained with PBE is shown in Figure 2 in comparison to the IR spectrum of a free water molecule calculated in the

same procedure. The spectrum is composed of a symmetrical (ν_1 stretch at ≈ 3630 cm^{-1}) and an antisymmetrical (ν_3 at ≈ 3760 cm^{-1}) band. It is worth emphasizing the red shift of both vibrational bands and the considerable increase of band intensities as a result of the adsorbed N_2 molecule; compare Table 1.

The performance of the chosen DFT functionals can be assessed on the basis of data presented in Table 1, with the MP2 results taken as a reference. The selected geometrical, energetical, and vibrational properties describe the weak interaction between water and nitrogen molecules. The relevant geometrical parameters are the hydrogen-bonding distance d(H—N) and angle α(O—H—N). The crucial vibrational properties are determined by the two harmonic stretching modes of water (with frequency shifts $\Delta\nu_{\text{sym}}$ and $\Delta\nu_{\text{anti}}$) delivering the model of the dangling OH band in water clusters.

It seems that the H—N bond length is slightly underestimated by PBE and overestimated by B3LYP in comparison to MP2. Using BHandH, we find a bond length deviation being an order of magnitude larger ($\delta = 0.28$ Å). The O—H—N angle is obtained with errors of $\delta = 0°$, $-2°$, and $15°$ for PBE, B3LYP, and BHandH, respectively. For the antisymmetric red-shift $\Delta\nu_{\text{anti}}$ and the relavite intensity $I_N/I_{W_{\text{anti}}}$, we find that B3LYP gives the smallest deviations of $\delta = -1$ cm^{-1} and $\delta = 0.1$, while PBE and BHandH show deviations of $\delta = 2$ and 4.5 cm^{-1} for the shift and of $\delta = 0.4$ and 0.3 for the relative intensity with respect to the MP2 results. The same trend is true for the symmetric red shift.

We further compare the binding energy of N_2—H_2O as shown in Table 2 between several methods and basis sets. For each method the geometry was optimized with the 6-311+G(d,p) basis set. On top of the energetically relaxed structures single-point calculations for a series of Dunning's basis sets has been carried out. For CCSD, the most accurate method in our test, the binding energy decreases slightly with growing basis set and does not seem to be fully converged even for the aug-cc-pV5Z basis set, reaching a value of -0.94 kcal/mol. On the other hand, the counterpoise corrected calculation with aug-cc-pV5Z gives a value of -0.89 kcal/mol which is quite similar such that we consider a value within this small range as our best reference. Both, B3LYP and PBE yield very good results in comparison to that reference value. While B3LYP rather underestimates the binding of water and dinitrogen, PBE overestimates it slightly.

Additionally a comparison of PBE and B3LYP was carried out also for larger test systems, namely, the first 10 lowest-energy clusters composed of 10 water molecules as found by Kazimirski and Buch.[18] Since CCSD is computationally prohibitive for these systems, we used MP2 as reference in that case. PBE underestimates the binding energies in comparison to MP2, and B3LYP does so slightly more. However, the results for both functionals are very similar. Considering the fact that MP2 overestimates the binding energy of N_2—H_2O as shown in Table 2 PBE and B3LYP seem equally adequate for our purpose. We decided to use GGA functional PBE because of the rather practical reason, the lower computational cost in comparison to the hybrid functional B3LYP which becomes particularly relevant for the larger water clusters.

In order to put our chosen DFT method to the acid test, we additionally took a deeper look at the relevant diagonal and off-diagonal terms of the Hessian matrix. At the MP2/aug-cc-pVTZ level of theory, the addition of one moiety N_2 to H_2O does not change the corresponding diagonal relaxed force constant[46]

6220

dx.doi.org/10.1021/jp111481q |*J. Phys. Chem. A* 2011, 115, 6218–6225

Table 1. Geometrical, Energetical, and Vibrational Properties^a of the Test System $(N_2)(H_2O)$ Obtained at Various Levels of Theory; 6-311+G(d,p) Basis Set Used for All Cases

	d(H−N) (Å)	α(O−H−N) (deg)	ΔE (kcal/mol)	ΔE^{BSSE} (kcal/mol)	$\Delta\nu_{sym}$ (cm^{-1})	$\Delta\nu_{anti}$ (cm^{-1})	$I_N/I_{W_{sym}}$	$I_N/I_{W_{anti}}$
MP2	2.39	175	−1.47	−1.00	2	6.5	2.8	1.9
PBE	2.35	175	−1.39	−1.17	6	8.5	6.6	2.3
B3LYP	2.41	177	−0.98	−0.81	4.5	7.5	3.9	2.0
BHandH	2.11	160	−2.73	−2.45	8.5	11	3.8	2.2

^{a} d(H−N), distance between H and N; α(H−O−N), angle between H, O, and N; ΔE, binding energy at 0 K calculated as the difference of potential energies $\Delta E = E^{H_2O-N_2} - E^{H_2O} - E^{N_2}$, no zero-point correction is included; ΔE^{BSSE}, counterpoise corrected binding energy;[45] $\Delta\nu$, red shift of vibrational frequency; I_N/I_W, intensity of vibrational band in the water−dinitrogen spectrum relative to the spectrum of the bare water molecule.

Table 2. Binding Energies (kcal/mol) for the Test System $(N_2)(H_2O)$ Calculated with Various Methods and Basis Sets^a

	MP2	CCSD	HF	B3LYP	PBE
optimization					
6-311+G(d,p)	−1.47	−1.29	−0.76	−0.98	−1.39
single point					
aug-cc-pVDZ	−1.54	−1.71	−0.54	−0.86	−1.26
aug-cc-pVTZ	−1.53	−1.27	−0.55	−0.79	−1.16
aug-cc-pVQZ	−1.40	−1.05	−0.51	−0.78	−1.17
aug-cc-pV5Z	−1.31	−1.94	−0.50	−0.75	−1.12
aug-cc-pVDZ-CP	−1.03	−1.24	−0.45	−0.68	−1.06
aug-cc-pVTZ-CP	−1.17	−0.94	−0.48	−0.72	−1.09
aug-cc-pVQZ-CP	−1.22	−0.91	−0.49	−0.74	−1.11
aug-cc-pV5Z-CP	−1.23	−0.89	−0.50	−0.74	−1.11

^{a} Geometry was optimized using the respective level of theory with the 6-311+G(d,p) basis set. At these geometries, single-point calculations were carried out with a series of Dunning's basis sets; additionally BSSE corrected values were calculated using the counterpoise correction scheme (−CP).

both, for the companion O−H band (8.33 N/m vs 8.34 N/m for PBE/6-311+G(d,p)) and the dangling O−H band (8.33 N/m vs 8.35 N/m). Nevertheless, our inspection of the relevant coupling terms, which are most susceptible for the quality of our simulations, revealed a sensible—and most important—negative coupling of the N_2−H_2O stretch with the dangling O−H coordinate (−0.050 N/m). In contrast, the coupling term between the N_2−H_2O stretching and the companion O−H coordinate is positive (+0.012 N/m). It is very encouraging that the DFT model is able to reproduce the relevant terms qualitatively and quantitatively: At the PBE level of theory both values are computed to be −0.053 and +0.011 N/m, respectively.

In the final benchmark step, we compared several basis sets for use with the PBE functional and found that it is essential to include diffuse functions in the basis set, while neither polarization functions nor passing from a double-ζ basis set to triple-ζ played such an important role. The details of comparison of the basis sets are provided in the Supporting Information. Finally, we decided to use the PBE functional with the 6-31+G(d) basis set, as this combination exhibits the best performance/cost ratio. With PBE/6-31+G(d), the binding energy of the test system $(N_2)(H_2O)$ is −1.48 kcal/mol, thus slightly overestimating the binding energy in comparison to the CCSD value (Table 2).

In order to obtain the IR spectra for the water clusters $(H_2O)_{10}$, $(H_2O)_{15}$, $(H_2O)_{20}$, and $(H_2O)_{30}$ as well as for the nitrogen-covered analogue (see Figure 1), we performed gas phase geometry optimizations (at 0 K with PBE/6-31+G(d)) of the first 10 lowest-energy structures taken from ref 18. The largest clusters treated in this work, which are necessary to compare the experimental and calculated spectra, are those composed of 30 water molecules covered with five to nine dinitrogen molecules $(N_2)_{5-9}(H_2O)_{30}$. The next biggest treated N_2-covered clusters are $(N_2)_{4-6}(H_2O)_{20}$.

The N_2-covered clusters were created by adding a N_2 molecule to every dangling O−H bond, oriented linearly in the direction of this O−H bond. For all optimized structures, IR spectra were computed using the normal-mode analysis with harmonic approximation as available in the Gaussian03 software package. (The gained harmonic frequencies were not scaled.) The theoretical spectra for every structure of a given cluster were extracted from the Gaussview3[47] program and then averaged; the resulting averaged spectra were finally visualized with Molden.[48] Due to the rapid cooling and nucleation of the water molecules out of the gas phase, the forming water particles are in fact in *thermal* equilibrium (compared to particles forming in supersonic jet expansions) but not in completed *thermodynamic* equilibrium. Therefore, a strictly Boltzmann weighted average is not feasible for the calculated spectra to fit the experimental spectra, and we decided to take the simplest approach of equal weighing.

■ RESULTS

Experimental Results. One experimental goal was to minimize the size of water clusters to allow a comparison (a) with water clusters generated by other techniques as supersonic jet-expansion[49−51] and (b) predominantly in this work with the computed water clusters, which are limited here to a maximum size of 30 molecules per cluster. This was accomplished by using low water sample gas concentrations and low buffer gas temperatures. The mean size of the nanoparticles is estimated by the following criteria: the position of the absorption maximum, an empiric criterion described by Devlin;[36] the ratio of the integrated absorbance of the bonded−OH band to the free−OH band; the occurrence of spectral substructure;[36] the comparison with other experimental results as, e.g., the data from helium beam scattering experiments combined with IR photodissociation;[7,51] comparison with previous calculations, also those of OH-stretch frequencies;[18,36] the comparison with ab initio calculations in refs 7 and 8 and this work, especially for spectra 5 and 6 in Figure 3. Especially the first, second, and last criteria have been used in this work.

In Figure 3, the IR spectra (i.e., the combined vibrational ν_1, ν_3 band) of pure water clusters at 80 K and N_2-covered water clusters at 5 K are compared. The spectra of clusters with partial or total N_2 covering are marked in blue in Figure 3, Figure 4a, and
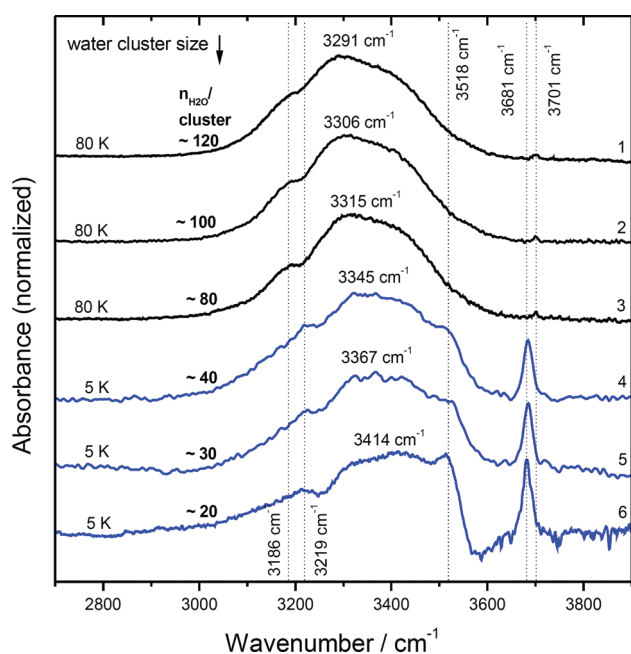
Figure 3. Dependence of the water O–H stretch band complex on the size of water cluster ranging from about 120 molecules to low tens. The estimated average size is given in the second column. Peak positions are indicated in cm^{-1}. The upper spectra (indicated with 1, 2, 3 in the last column) are recorded in this work and are due to freely suspended pure water clusters in thermal equilibrium; the lower spectra (indicated with 4, 5, and 6) are due to N$_2$-covered water clusters at 5 K and are taken from a previous work for comparison.[36].

Figure 4. The transition from bare to N$_2$-covered water particles. (a) Dependence on water concentration: FTIR spectra of water clusters formed at ca. 5 K with decreasing water concentration (from top to bottom). A new band at 3676 cm^{-1} develops with increasing relative nitrogen concentration. (b) Dependence on temperature: The water clusters decrease in size with temperature dropping from 80 to 20 K. The onset of nitrogen adsorption on the particle surface (red shift and increase of intensity of the free OH band) occurs at about 30 K. Note that Devlin et al. found the onset for mobilization of N$_2$ adsorbed at a microporous amorphous ice surface at 18 K.[52] All spectra shown in this figure are recorded in the present work.

Figure 4b (spectra 4, 5, 6, 8, 9, 10, 14, and 15). The spectra at 80 K (1, 2, 3) probably represent the smallest pure water clusters recorded in thermal equilibrium, consisting of 80 to 120 molecules. Compared to spectrum 7 in Figure 4 recorded for water clusters of similar size but generated at 5 K, the spectra at 80 K show a shoulder at 3186 cm^{-1}, which could be a hint for a higher degree of crystallinity favored at the higher temperature. In Figure 4, the transition from pure to N$_2$ covered water clusters is presented, which was achieved by the reduction of (a) the water (particle) concentration of the sample gas relative to the nitrogen concentration and (b) the buffer-gas temperature in the cooling cell. The N$_2$ concentration was about 10–100 times lower than the water (particle) concentration. Note that in Figure 4a, two distinct free–OH bands can be detected in the transition spectra 8 and 9, at 3676 and 3702 cm^{-1}. In the case of Figure 4b, spectrum 14 marks incomplete N$_2$ covering, and the free–OH band of the N$_2$ covered clusters starts to appear at 3675 cm^{-1}. Our interpretation is that there is an onset of nitrogen adsorption at the water cluster surfaces roughly at 30 K for cluster sizes of about 100 water molecules. These results are in accordance with the observations and experiments by Devlin et al. carried out for large water ice clusters and deposited amorphous ice combined with various adsorbates.[2,52,53]

Computational Results. For each of the 10 lowest energy structures, for every cluster size (H$_2$O)$_{10}$, (H$_2$O)$_{15}$, (H$_2$O)$_{20}$, and (H$_2$O)$_{30}$ as well as for each N$_2$-covered counterpart, an IR spectrum was calculated (that means 80 spectra in total). Ten spectra for every cluster size have been averaged to yield one spectrum for every cluster size, both bare and N$_2$ covered. Figure 5 shows two IR spectra for each of the four cluster sizes.
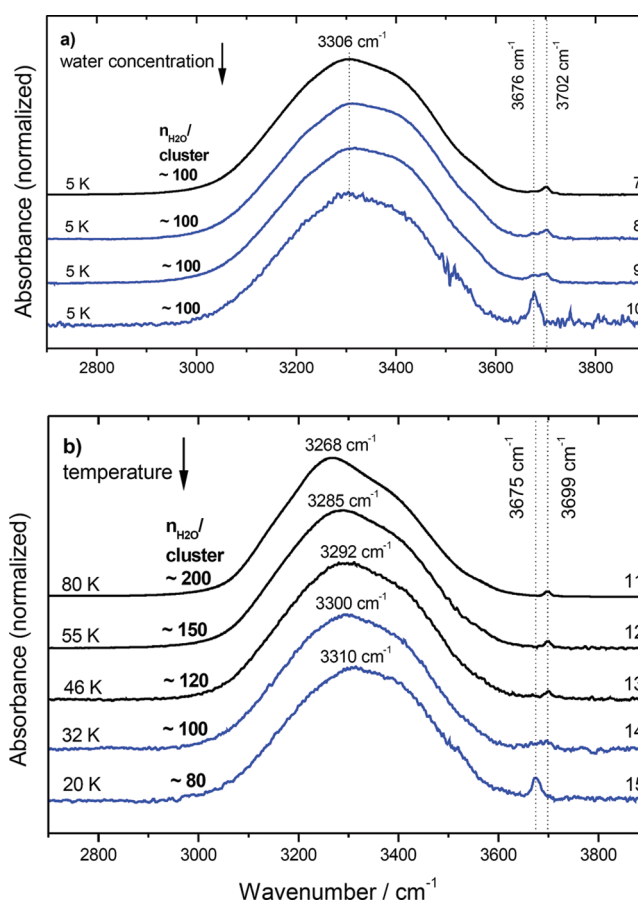
The solid red curve indicates the averaged IR spectrum of the uncovered water clusters, and the dashed blue spectrum was obtained for the N$_2$-covered water clusters.

The shown spectra in Figure 5 containing 10 (a), 15 (b), 20 (c), and 30 (d) water molecules were generated by averaging 10 single spectra of 10 configurations for each water cluster size. The computed frequencies and intensities were processed with the Gaussview3 program[47] to yield IR spectra, assuming a Gaussian shape for the vibrational bands. The spectra for the individual structures (isomers) of every water cluster were averaged simply by summing them and dividing by 10, the number of available spectra.

Comparing the four pairs of spectra in Figure 5, a number of results can be concluded depending on the cluster size and on the degree of N$_2$ covering. First, a tendency of spectral change can be observed starting with band centers at 2900 and 3400 cm^{-1} for the smaller clusters including 10 water molecules (see Figure 5a) toward a spectral shape with an increasing dominating center-band region around 3200 cm^{-1} (see panels b–d of Figure 5). This reflects the relative increase of four-coordinated water
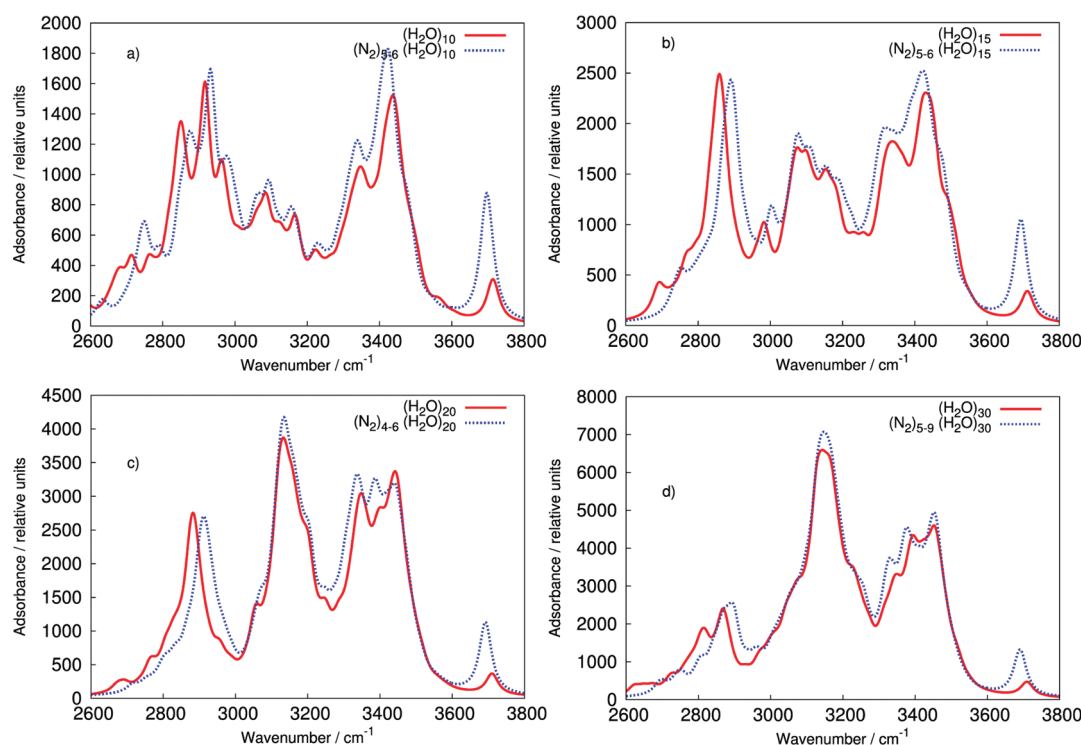
Figure 5. Ab initio calculated IR spectra of the OH-stretch region of pure and nitrogen-covered water clusters with 10, 15, 20, and 30 water molecules. (a) $(H_2O)_{10}$ cluster spectra (red and solid lines) and $(N_2)_{5-6}(H_2O)_{10}$ cluster spectra (blue and dashed lines); (b) $(H_2O)_{15}$ and $(N_2)_{5-6}(H_2O)_{15}$ cluster spectra; (c) $(H_2O)_{20}$ and $(N_2)_{4-6}(H_2O)_{20}$ cluster spectra; (d) $(H_2O)_{20}$ and $(N_2)_{5-9}(H_2O)_{20}$ cluster spectra. For each of the four cluster sizes 10 spectra of minimum energy structures of pure/N_2-covered clusters have been averaged. Compare Figure 1 as an example of N_2 coating. The spectra are visualized with the Molden program.

Table 3. Nitrogen Molecules Adsorbed on the Water Clusters Cause Two Effects Both in Computations and in the Experiment: a Red Shift $\Delta\nu$ and a Relative Intensity I_N/I_W Increase of the Free O—H Band at around 3700 cm^{-1}

cluster	$\Delta\nu$ (cm^{-1})	I_N/I_W
$(N_2)_{5-6}(H_2O)_{10}$	17	2.8
$(N_2)_{5-6}(H_2O)_{15}$	18	3.1
$(N_2)_{4-6}(H_2O)_{20}$	18	3.1
$(N_2)_{5-9}(H_2O)_{30}$	19	2.8
experiment/this work (80—200 water molecules), see Figure 4	24—26	3—4
experiment/this work (20—40 water molecules), see Figure 3	18—21	

molecules within the clusters (which absorb in the band center region) with increasing cluster size compared to water molecules at the surface.[18,36] In the same way, the decrease of both (a) the "companion" O—H band at 2900 cm^{-1} and (b) the "dangling" O—H band at 3700 cm^{-1} which are due to the bonded and the free O—H vibration of three-coordinated water molecules with a free O—H band can be explained by a relative decrease of numbers of surface water molecules with increasing cluster size.[18,36] Note that the companion band at the PBE/6-31+G(d) level of theory is obtained at lower frequencies in comparison to the semiempirical calculations of ref 36 with the TIP4P force field where it was obtained at about 3100 cm^{-1}. The experimental value as shown in Figure 3 is even higher at about 3200 cm^{-1}. Second, the effect of the N_2 molecules adsorbed at the surface of the water clusters seems to be not very strong in the spectral region between 2600 and 3600 cm^{-1} presented in Figure 5. A tendency of a blue shift of the "companion" O—H band region around 2900 cm^{-1} can be observed. The strongest impact of the

adsorbed nitrogen on the spectra can be seen for the "dangling" free O—H band at around 3700 cm^{-1}. For all four cluster sizes two effects are obvious: a red shift of this band by around 20 cm^{-1} and an increase of the band intensity by roughly a factor of 3. In Table 3, both effects are described in detail.

■ DISCUSSION AND CONCLUSIONS

In Table 3 the red shift and the relative intensity increase of the free O—H band are depicted both for the computational results and for the experimental results. Note that the smallest pure water clusters which could be generated in our experiment were about 80 water molecules compared to the smallest nitrogen-covered water clusters which consist of a core of about 20 water molecules; see Figure 3. Therefore, in the experimental case the experimental spectra of N_2-covered and uncovered water clusters cannot be directly compared for the smaller sizes (20—40 water molecules) as in the computational case. Nevertheless, in the experimental spectra the O—H band position of the pure water

clusters is considerably stable for all experiments and concentrates in the range between 3699 and 3702 cm^{-1} (see Figure 4). Therefore, a red shift of 18–21 cm^{-1} for the smaller nitrogen-covered water clusters can be concluded for the experimental spectra. This is in nice agreement with the computational results listed in Table 3 ranging between 17 and 19 cm^{-1}. Even the tendency toward an increase of the red shift with increasing cluster size can be observed both for the experimental (24–26 cm^{-1}, 80–200 molecules) and for the computational (17–19 cm^{-1}, 10–30 molecules) results.

Typically the harmonic approximation yields frequencies, which overestimate the experimental frequencies by several hundred wavenumbers. This is clearly due to the lack of anharmonic contributions in the harmonic theory. However, it is known in literature (see ref 54 and references therein) that GGA density functionals such as PBE systematically underestimate the harmonic frequencies and therefore yields frequencies, which are in good agreement with the experimental frequenices with errors below 10%.

Also the relative intensity increase of the free O−H band due to nitrogen adsorption is in good agreement if one compares the experimental and computed spectra for the comparable sizes of 20–30 water molecules; see Table 3. Independent of the cluster size the intensity increase of the dangling−OH band stays nearly constant for the different cluster sizes in the range of 2.8–3.1. Obviously the change of dipole moment along the respective normal mode coordinate is different for pure and N$_2$ covered clusters, which results in the increased infrared intensity.

If one compares the experimental spectra with the calculated spectra, one has to take into account that in the experimental case one observes a spectral average of a cluster size-distribution around a mean size value and, furthermore, that much more than 10 cluster structures contribute to the experimental average spectrum compared to the corresponding computed average spectrum. Both lead to a stronger smoothing effect in the resulting average spectra in the experimental case. Nonetheless, the comparability of experimental and computed spectra of nitrogen-covered water clusters of the same average size is surprisingly good (e.g., compare spectrum 5 of Figure 3 with the blue spectrum of Figure 5d).

While the experimental nitrogen-covered water cluster size was limited for our collisional cooling technique to a minimum average size of 30, on the other hand there is an upper limit for accurate ab initio/DFT calculation with justifiable computation costs to about 30 to 50 water molecules. Therefore, in a way we successfully realized an overlap of experimental and computational facilities in the present work.

ASSOCIATED CONTENT

S **Supporting Information.** Tables showing the binding energies of (N$_2$)(H$_2$O) calculated for different basis sets using the PBE functional, geometrical, energetical, and vibrational properties of (N$_2$)(H$_2$O), binding energies per N$_2$ molecule in the N$_2$ covered water cluster, and characteristics of the averaged spectra of the water clusters calculated at the PBE/6-31+G(d) level of theory. This material is available free of charge via the Internet at http://pubs.acs.org.

AUTHOR INFORMATION

Corresponding Author
*E-mail: for computational materials, marcus.elstner@kit.edu; for experimental issues, s.bauerecker@tu-braunschweig.de.

REFERENCES

(1) Barnes, A. J. In *Vibrational Spectra of Trapped Species*; Hallam, H. E., Ed.; Wiley: New York, 1973; Chapter on the theoretical analysis of frequency shifts.

(2) Sadlej, J.; Rowland, B.; Devlin, J. P.; Buch, V. *J. Chem. Phys.* **1995**, *102*, 4804.

(3) Devlin, J. P.; Buch, V. *J. Phys. Chem. B* **1997**, *101*, 6095.

(4) Devlin, J. P.; Buch, V. In *Water in Confining Geometries*; Buch, V., Devlin, J. P., Eds.; Springer: Berlin, 2003; Ice nanoparticles and ice adsorbate interactions: FTIR spectroscopy and computer simulations, p 425.

(5) Sandler, P.; Oh Jung, J.; Szczęśniak, M. M.; Buch, V. *J. Chem. Phys.* **1994**, *101*, 1378.

(6) Kuma, S.; Slipchenko, M. N.; Kuyanov, K. E.; Momose, T.; Vilesov, A. *J. Phys. Chem. A* **2006**, *110*, 10046.

(7) Buck, U.; Ettischer, I.; Melzer, M.; Buch, V.; Sadlej, J. *Phys. Rev. Lett.* **1998**, *80*, 2578.

(8) Sadlej, J.; Buch, V.; Kazimirski, J. K.; Buck, U. *J. Phys. Chem. A* **1999**, *103*, 4933.

(9) Buck, U.; Meyer, H. *J. Chem. Phys.* **1986**, *84*, 4854.

(10) Buck, U. *J. Phys. Chem.* **1994**, *98*, 5190.

(11) Xantheas, S. S. *J. Chem. Phys.* **1995**, *102*, 4505.

(12) Hartke, B. *Phys. Chem. Chem. Phys.* **2003**, *5*, 275.

(13) Hartke, B. *Eur. Phys. J. D* **2003**, *24*, 57.

(14) Hartke, B. *Angew. Chem., Int. Ed.* **2002**, *114*, 1534.

(15) Jorgensen, W. L.; Chandrasekhar, J.; Madura, J. D.; Impey, R. W.; Klein, M. L. *J. Chem. Phys.* **1983**, *79*, 926.

(16) Burnham, C. J.; Xantheas, S. S. *J. Chem. Phys.* **2002**, *116*, 5115.

(17) Lagutschenkov, A.; Fanourgakis, G. S.; Niedner-Schatteburg, G.; Xantheas, S. S. *J. Chem. Phys.* **2005**, *122*, 194310.

(18) Kazimirski, J. K.; Buch, V. *J. Phys. Chem. A* **2003**, *107*, 9762.

(19) Ireta, J.; Neugebauer, J.; Scheffler, M. *J. Phys. Chem. A* **2004**, *108*, 5692.

(20) Santra, B.; Michaelides, A.; Scheffler, M. *J. Chem. Phys.* **2007**, *127*, 184104.

(21) Elstner, M.; Hobza, P.; Frauenheim, T.; Suhai, S.; Kaxiras, E. *J. Chem. Phys.* **2001**, *114*, 5149.

(22) Wu, Q.; Yang, W. *J. Chem. Phys.* **2002**, *116*, 515.

(23) Grimme, S. *J. Comput. Chem.* **2004**, *25*, 1463.

(24) Grimme, S.; Antony, J.; Ehrlich, S.; Krieg, H. *J. Chem. Phys.* **2010**, *132*, 154104.

(25) Xu, X.; Goddard, W. A., III *J. Chem. Phys.* **2004**, *121*, 4068.

(26) Xu, X.; Goddard, W. A., III *Proc. Natl. Acad. Sci. U.S.A.* **2004**, *101*, 2673.

(27) Zhao, Y.; Truhlar, D. G. *J. Chem. Theory Comput.* **2006**, *2*, 1009.

(28) Palermo, N. Y.; Csontos, J.; Owen, M. C.; Murphy, R. F.; Lovas, S. *J. Comput. Chem.* **2007**, *28*, 1208.

(29) Bauerecker, S.; Taucher, F.; Weitkamp, C.; Michaelis, W.; Cammenga, H. K. *J. Mol. Struct.* **1995**, *348*, 237.

(30) Bauerecker, S.; Taraschewski, M.; Weitkamp, C.; Cammenga, H. K. *Rev. Sci. Instrum.* **2001**, *72*, 3946.

(31) Taraschewski, M.; Cammenga, H. K.; Tuckermann, R.; Bauerecker, S. *J. Phys. Chem. A* **2005**, *109*, 3337.

(32) Bauerecker, S. *Phys. Rev. Lett.* **2005**, *94*, 033404.

(33) Dartois, E.; Bauerecker, S. *J. Chem. Phys.* **2008**, *128*, 154715.

(34) Rowland, B.; Devlin, J. P. *J. Chem. Phys.* **1991**, *94*, 812.

(35) Bauerecker, S.; Wargenau, A.; Schultze, M.; Kessler, T.; Tuckermann, R.; Reichardt, J. *J. Chem. Phys.* **2007**, *126*, 134711.

(36) Buch, V.; Bauerecker, S.; Devlin, J. P.; Buck, U.; Kazimirski, J. K. *Int. Rev. Phys. Chem.* **2004**, *23*, 375.

6224

dx.doi.org/10.1021/jp111481q |*J. Phys. Chem. A* 2011, 115, 6218–6225

(37) Becke, A. D. *J. Chem. Phys.* **1993**, *98*, 5648.

(38) Becke, A. D. *J. Chem. Phys.* **1993**, *98*, 1372.

(39) Perdew, J. P.; Burke, K.; Ernzerhof, M. *Phys. Rev. Lett.* **1996**, 77, 3865.

(40) Zhao, Y.; Truhlar, D. G. *J. Chem. Theory Comput.* **2005**, *1*, 415.

(41) Rao, L.; Ke, H.; Fu, G.; Xu, X.; Yan, Y. *J. Chem. Theory Comput.* **2009**, *5*, 86.

(42) Boys, S. F.; Bernardi, F. *Mol. Phys.* **1970**, *19*, 553.

(43) Frisch, M. J. et al. *Gaussian 03, Revision C.02*, Gaussian, Inc.: Wallingford, CT, 2004.

(44) Møller, C.; Plesset, M. S. *Phys. Rev.* **1934**, *46*, 618.

(45) Van Duijneveldt, F. B.; Van Duijneveldt-Van De Rijdt, J.; Van Lenthe, J. H. *Chem. Rev.* **1994**, *94*, 1873.

(46) Brandhorst, K.; Grunenberg, J. *Chem. Soc. Rev.* **2008**, *37*, 1558.

(47) Dennington II, R.; Keith, T.; Eppinnett, K.; Hovell, W. L.; Gilliland, R. *GaussView; Technical Report*, 2000

(48) Schaftenaar, G.; Noordik, J. H. *J. Comput.-Aided Mol. Des.* **2000**, *14*, 123.

(49) Devlin, J. P.; Fárnk, M.; Suhm, M. A.; Buch, V. *J. Phys. Chem. A* **2005**, *109*, 955.

(50) Liu, Y.; Weimann, M.; Suhm, M. A. *Phys. Chem. Chem. Phys.* **2004**, *6*, 3315.

(51) Buck, U.; Huisken, F. *Chem. Rev.* **2000**, *100*, 3863.

(52) Devlin, J. P.; Silva, S. C.; Rowland, B.; Buch, V. In *Hydrogen bond networks*; Bellisent-Funel, M.-C., Dore, J. C., Eds.; Kluwer Academic Publishers: Dordrecht and Boston, 1994; Spectroscopic and simulation study of ice surfaces: bare and with adsorbates, p 373.

(53) Rowland, B.; Fisher, M.; Devlin, J. P. *J. Chem. Phys.* **1991**, *95*, 1378.

(54) Neese, F. *Coord. Chem. Rev.* **2009**, *253*, 526.

6225

dx.doi.org/10.1021/jp111481q |*J. Phys. Chem. A* 2011, 115, 6218–6225